Available online at www.sciencedirect.com
ScienceDirect
Vision Research 47 (2007) 1608–1613
Vision Research
www.elsevier.com/locate/visres

Cortical specialization for concentric shape processing

Serge O. Dumoulin *, Robert F. Hess

McGill Vision Research Unit, Department of Ophthalmology, McGill University, Montréal, Canada

Received 7 July 2006; received in revised form 24 November 2006

Abstract

It is current dogma that neurons in primary visual cortex extract local edges from the scene, from which later visual areas reconstruct more meaningful shapes. In intermediate areas, such as area V4, responses are driven by features more complex than local oriented edges but more basic than meaningful shapes. The present study was motivated by the proposal that concentric (circular) shape processing is an important aspect of intermediate shape processing and is proposed to occur in area V4. However, previous studies are not able to discriminate between the number of orientations within the image nor how these orientations vary across space (orientation gradient, contrast or curvature) as opposed to concentric shape processing *per se*. We address the question whether V4 responses are driven by curvature or circularity. We use fMRI and tightly controlled narrowband stimuli with identical local and global properties. These patterns either form random or circular patterns with tightly matched orientation gradients and therefore similar curvature. We find stronger responses to circular patterns in areas V3/VP and V4. Our results suggest that extracting circular shape is an important step in intermediate shape processing.

Keywords: Functional brain imaging; fMRI; Spatial vision; Form vision; Curvature

1. Introduction

A crucial role of our visual system is to detect and segregate objects. In primary visual cortex (V1) local, oriented edges from the visual scene are extracted (Hubel & Wiesel, 1959, 1962), and V1 has been considered as a bank of oriented filters (De Valois & De Valois, 1988). These filters are the basis of shape perception, from which later visual areas reconstruct more meaningful objects. In intermediate areas, such as area V4, responses are driven by features more complex than local oriented edges but more basic than meaningful objects (Desimone & Schein, 1987; Gallant, Braun, & Van Essen, 1993; Gallant, Connor, Rakshit, Lewis, & Van Essen, 1996; Pasupathy & Connor, 1999, 2001, 2002; Pollen, Przybyszewski, Rubin, & Foote, 2002; Schiller & Lee, 1991).

The present study was motivated by the proposal that concentric (circular) shape processing is an important aspect of intermediate shape processing and is proposed to occur in area V4 (Gallant et al., 1993, 1996; Wilkinson et al., 2000; Wilson, Wilkinson, & Asaad, 1997; Wilson & Wilkinson, 1998). This hypothesis is supported by electrophysiological studies describing neurons that respond at least twice as strong to concentric, radial or hyperbolic stimuli than to 1D sinusoidal (parallel) gratings in macaque V4 (Gallant et al., 1993, 1996). Human event-related potentials (ERP) have also reported stronger responses to concentric and radial shapes than to parallel patterns (Pei, Pettet, Vildavski, & Norcia, 2005). The importance of concentric shape processing is further supported by human psychophysics, where sensitivity to shape discrimination has been reported to be the highest for circular shape (Achtman, Hess, & Wang, 2003; Hess, Wang, & Dakin, 1999; Kurki & Saarinen, 2004; Levi & Klein, 2000; Wilson et al., 1997; Wilkinson, Wilson, & Habak, 1998), and sensitivity to closed contours is much higher than nonclosed contours (Kovács & Julesz, 1993). This hypothesis is

* Corresponding author. Present address: Department of Psychology, Stanford University, Stanford, USA.
E-mail address: serge.dumoulin@stanford.edu (S.O. Dumoulin).

0042-6989/$ - see front matter © 2007 Elsevier Ltd. All rights reserved.
doi:10.1016/j.visres.2007.01.031

further supported by a study of a patient with a lesion around area V4 that is deficient in concentric shape processing (Gallant, Shoup, & Mazer, 2000). Lastly, using functional magnetic resonance imaging (fMRI) Wilkinson et al. (2000) reported that human V4 responded stronger to concentric and radial shapes than to parallel patterns, confirming the importance of concentric shape processing in humans.

On the other hand, concentric and parallel patterns differ in a number of image properties, such as number of orientations and how these orientations vary across space, either semi-randomly (orientation contrast) or smoothly (curvature). Therefore, these previous studies cannot discriminate between number of orientations, orientation contrast or curvature as opposed to concentric shape processing *per se*. Early visual cortex is known to be modulated by orientation contrast (Allman, Miezin, & McGuinness, 1985; Dumoulin & Hess, 2006; Fitzpatrick, 2000; Kastner, Weerd, & Ungerleider, 2000; Williams, Singh, & Smith, 2003; Zenger-Landolt & Heeger, 2003), and curvature has been proposed to be a critical tuning dimension for early visual cortex (e.g. V2 Ito & Komatsu, 2004) and in particular V4 (Pasupathy & Connor, 1999, 2001, 2002; Pollen et al., 2002). In support of the importance of curvature rather than circularity, psychophysical studies have suggested that it is the curvature smoothness rather than contour closure that is the important factor for determining contour saliency (Hess & Field, 1999; Pettet, McKee, & Grzywacz, 1998). In addition, it has been suggested that some of the psychophysical results indicating higher sensitivity to concentric patterns using rotational glass patterns (Wilson et al., 1997; Wilson & Wilkinson, 1998) may have been influenced by stimulus windowing rather than concentric processing *per se* (Dakin & Bex, 2002), although this has been challenged in an ERP study (Pei et al., 2005). Finally, the patient deficient in concentric shape discrimination was also deficient in curvature perception (Gallant et al., 2000). Therefore, the key question that we address is: is this proposed concentric shape processing driven by concentric structure or more general image properties such as curvature?

Second, in their fMRI study, Wilkinson et al. (2000) only showed data limited to V1, V4 and a region particularly responsive to viewing of faces (fusiform face area; FFA; Kanwisher, McDermott, & Chun, 1997). A similar argument holds for the electrophysiological studies that are limited by the cortical sampling of neurons. Therefore, these previous studies do not establish whether any concentric shape processing is limited to V4. So the second aim of this study is to assess whether any specialization for processing concentric shape is limited to area V4.

We use fMRI and tightly controlled narrowband stimuli composed of Gabors (Achtman et al., 2003; Dumoulin & Hess, 2006) to address these issues. The Gabors were arranged to create either non-circular patterns or circular patterns. These patterns are matched both locally and globally in terms of total orientations and how orientations are distributed across space (orientation contrast and curvature) and thus allow us to address the as yet unanswered question of whether it is the orientation contrast/curvature or circularity that drives V4 responses.

2. Materials and methods

2.1. Subjects

Four experienced psychophysical observers were used as subjects (all male, mean age: 39, age range: 30–54). The subjects were instructed to fixate at a provided fixation-point and trained prior to the scanning session to familiarize them with the task. All observers had normal or corrected-to-normal visual acuity. All studies were performed with the informed consent of the subjects and were approved by the Montréal Neurological Institute Research Ethics Committee.

2.2. Visual stimuli

For a more detailed description of the stimuli see Dumoulin and Hess (2006). The visual stimuli were generated in the MatLab programming environment and displayed using the PsychToobox (Brainard, 1997; Pelli, 1997) on a Macintosh G4 Powerbook, and displayed on a LCD projector (NEC Multisync MT820). The visual display subtended 20 degrees (diameter).

The stimuli were constructed from 625 oriented Gabors, i.e. a 1D sine-wave enclosed in a 2D Gaussian envelope ($\lambda = 0.2$ and $\sigma = 0.1$ degrees), i.e. the spatial frequency content of the images was centered on 5 cycles/degree. The positions of the Gabors were jittered (−0.4 to 0.4 degrees) around a square grid centered on the image matrix (grid distance = 0.8 degrees). The contrast of each Gabor was randomly chosen from a uniform distribution (contrast range = 25–100%). The global orientation content was controlled to be isotropic between 0 and 360 degrees.

Two different stimuli types were used (see Fig. 1). In one stimulus type the Gabor array formed 10 circles with random centers (Fig. 1a), in the other the Gabors formed random arrays were the local orientation smoothness or contrast was constrained to be similar to the circular shapes (Fig. 1b; for more detail on the creation of these images see Appendix A). We will refer to these types of images as "circle" and "flowfield" images. The orientation difference of neighboring Gabors as a function of the Gabor euclidean distance was used to match the orientation gradient of the flowfield images to that of the circular images. The orientation gradient is identical between the two image types indicating that the stimuli have similar curvature (Fig. 1c). Therefore, the only difference between the stimulus conditions was the presence or absence of circular structure.

The different stimulus conditions were alternated in a block design (block duration 12 s). Each condition (block) was repeated at least five times giving a total duration of approximately 6 min per scan. The stimuli were presented time-locked to the acquisition of fMRI time-frames, i.e. every 3 s. To control for attention, the subjects continuously performed a two-interval forced-choice (2IFC) contrast-discrimination task. That is, a given stimulus presentation consisted of two intervals, both displaying a different image from the same condition either at full or reduced (0.7×) contrast. The subject indicated which interval contained the high contrast stimulus. Each image was presented for 500 ms and the inter-stimulus interval was 500 ms. In the remaining 1.5 s the subjects' responses were recorded. During mean luminance (blank) conditions an identical task was performed for the fixation dot. The subjects' performance was on average 75% correct.

2.3. Magnetic resonance imaging

The magnetic resonance images were acquired with a Siemens Sonata 1.5T MRI. The experiments were conducted with the subjects lying on their back with a surface-coil (circularly polarized, receive only) centered over their occipital poles. Head position was fixed by means of a foam head-rest and a bite-bar.

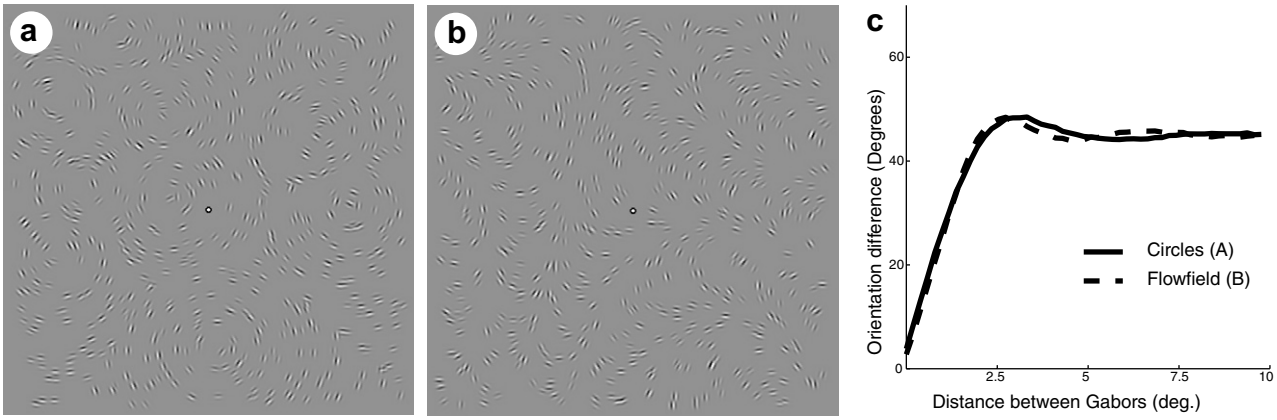

Fig. 1. Examples of the Gabor array stimuli used. The stimuli form either circles (a) or random "flowfield" patterns (b) where the curvature—defined as the orientation difference between neighboring Gabor elements (c)—is similar to that of the circular images.

Multislice T2*-weighted gradient echo (GE) echo-planar imaging (EPI) functional MR images (TR/TE = 3000/51 ms, flip angle = 90 degrees, #slices = 30 (contiguous), slice thickness = 4 mm) were acquired using a surface-coil (receive only) with a 64×64 acquisition matrix and a 256×256 mm rectangular field of view. The slices were taken parallel to the calcarine sulcus and covered the entire occipital and parietal lobes and large dorsal-posterior parts of the temporal and frontal lobes. One hundred and twenty eight measurements (time frames) were acquired. Ten to fourteen fMRI scans were performed in each session. T1-weighted anatomical MR images (aMRI) were acquired prior to the commencement of the functional scans. This aMRI utilized a 3D GE sequence (TR = 22 ms, TE = 9.2 ms, flip angle = 30 degrees, 256×256 mm rFOV) and yielded 80 sagittal images with a thickness of 2 mm.

In separate sessions T1-weighted aMRI images were acquired with a head-coil, also with a 3D GE sequence, yielding 160 sagittal images comprising 1 mm^3 voxels. Identification of the visual areas was also performed in another separate session with similar parameters.

2.4. Processing of anatomical images

The anatomical MRI scans were corrected for intensity non-uniformity (Sled, Zijdenbos, & Evans, 1998) and automatically registered (Collins, Neelin, Peters, & Evans, 1994) in a stereotaxic space (Talairach & Tournoux, 1988). The surface-coil aMRI, taken with the functional images, was aligned with the head-coil aMRI, thereby allowing an alignment of the functional data with a head-coil MRI and subsequently stereotaxic space (Collins et al., 1994; Dumoulin et al., 2000; Sled et al., 1998). The aMRIs were classified into gray-matter, white-matter and CSF (Cocosco, Zijdenbos, & Evans, 2003), after which two cortical surfaces were reconstructed at the inner and outer edge of the cortex (MacDonald, Kabani, Avis, & Evans, 2000). The surface-normals of the cortical models were smoothed to produce an 'unfolded' model of the cortical sheet (MacDonald et al., 2000).

2.5. Preprocessing of functional images

The first two time-frames of each functional run were discarded due to start-up magnetization transients in the data. All remaining time-frames were blurred with an isotropic 3D Gaussian kernel (full-width-half-maximum = 6 mm) to attenuate high frequency noise. The functional scans were corrected for subject motion within and between fMRI scans (Collins et al., 1994).

2.6. Identification of visual areas

Early visual cortical areas were identified using volumetric phase-encoded retinotopic mapping (Dumoulin et al., 2003). By combining eccentricity and polar-angle phase-maps (Engel et al., 1994) with the anatomical MRI, the visual field signs of different visual areas could be segmented. Neighboring visual areas could be identified due to opposite field signs; i.e. V1, V2, V3/VP, V3a and V4 (Dumoulin et al., 2003; Sereno et al., 1995).

2.7. Statistical analysis

The fMRI data were analyzed using software developed by Worsley et al. (2002). The statistical analysis is based on a linear model with correlated errors. Runs, sessions and subjects were combined using a linear model with fixed effects and standard deviations taken from the previous analysis on individual runs. A random effects analysis was performed by first estimating the ratio of the random effects variance to the fixed effects variance, then regularizing this ratio by smoothing it with a Gaussian filter to achieve 100 effective degrees of freedom. The variance of the effect was then estimated by the smoothed ratio multiplied by the fixed effects variance to achieve higher degrees of freedom. The resulting *t*-statistical images were thresholded for peaks and cluster sizes using random field theory (Worsley et al., 1996).

The volume-of-interest analysis (VOI) of the identified visual areas (V1–V4) was done in an identical fashion (Worsley et al., 2002). These visual areas were identified in each subject. Prior to the statistical analysis, the time-series were converted to percent BOLD signal change and all the time-series of voxels responding to all stimuli within a VOI (left and right hemispheres) were averaged together, with exclusion of voxels displaying artifacts. Because the time-series were converted to percent BOLD signal change prior to the analysis, the effect size of the linear model (β) is also in percent signal change. The differential effects sizes and their standard deviations, averaged across all subjects, are plotted in Fig. 3.

3. Results

In this experiment, we assessed whether there is a cortical specialization for processing circular shape. Our stimuli were tightly controlled for low-level statistics such as curvature. A statistical comparison between fMRI signals elicited by viewing of the circle and flowfield stimuli are shown in Fig. 2. This figure reveals stronger fMRI signals elicited by viewing of the circle images as compared to flowfield images in and around the average location of area V4.

In Fig. 2, the activation of both left and right pV4 reach significance. The peak *t*-statistical values are 5.62 and 7.16 at stereotaxic (Collins et al., 1994; Talairach & Tournoux, 1988) coordinates $[-26, -74, -8]$ and $[30, -78, -16]$ in the left and right hemisphere, respectively. These *t*-statistical

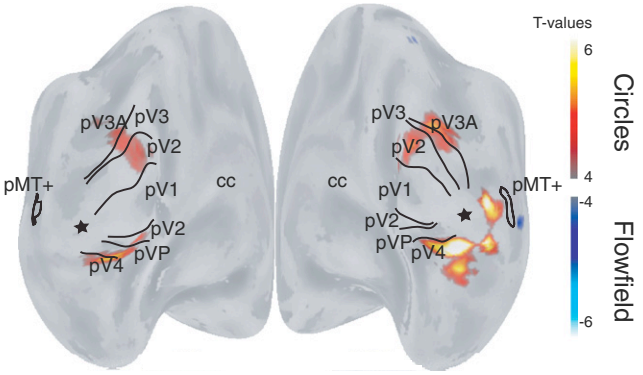

Fig. 2. Average t-statistical maps (4 subjects) displayed on their unfolded average cortical surfaces ($t = 5.2$ corresponds to $p = 0.05$ corrected for multiple comparisons). Stronger fMRI activations elicited by either viewing of circle or flowfield images are shown. Oblique posterior-medial views are shown of the left and right hemisphere. These views reveal all differential activations. The average borders of the visual areas are drawn by black lines, thereby illustrating the probabilistic (p) location of the visual areas. The foveal representation is indicated by a star and the corpus callosum (cc) is labeled. As can be seen from these t-statistical maps, selective activations to the circle images is found in and around pV4.

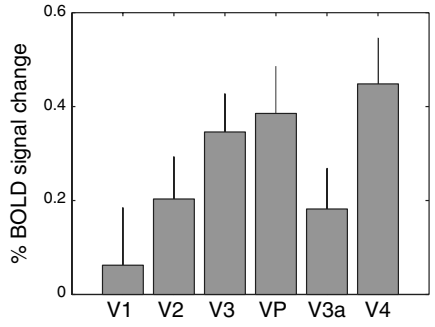

Fig. 3. Average differential BOLD signal amplitudes and standard deviations elicited by viewing circle versus flowfield images are plotted for the identified visual areas. The bar graph shows significantly (for t and p values see Table 1) stronger responses to viewing the circle versus flowfield images in areas V3/VP and V4.

values correspond to p-values smaller than <0.01 corrected for multiple comparisons (Worsley et al., 1996).

The observation that V4 is selectively activated by circular structure is confirmed in a VOI analysis (Fig. 3 and Table 1). In this VOI analysis, the early visual areas are identified in each subject individually using retinotopic mapping methodologies (Dumoulin et al., 2003). We find that both areas V3/VP and V4 are activated significantly stronger by viewing of circle versus flowfield images.

Table 1
t-values and corresponding p-values for the identified brain regions for a statistical comparison between the circle and flowfield images

Area	t (p)-value
V1	0.51 (>0.7)
V2	2.26 (0.08)
V3	4.27 (<0.001)
VP	3.83 (<0.001)
V3A	2.10 (0.12)
V4	4.56 (<0.001)

The p-values were Bonferroni corrected for the number of identified areas (6).

4. Discussion

We describe the fMRI BOLD signal changes elicited by the viewing of two different stimuli both constructed of Gabor arrays. In one stimulus the Gabor array formed 10 circles with random centers, whereas in the other the Gabors formed random arrays. In both cases the local orientation smoothness and gradient was identical and consequently the curvature was similar. We found stronger signals to the circular patterns in V3/VP and V4.

Attentional modulation can substantially affect neuroimaging responses in visual cortex (Beauchamp, Cox, & DeYoe, 1997; Brefczynski & DeYoe, 1999; Gandhi, Heeger, & Boynton, 1999; Martinez et al., 1999; O'Craven, Rosen, Kwong, Treisman, & Savoy, 1997; Somers, Dale, Seiffert, & Tootell, 1999) and could potentially confound the interpretation of the results. Therefore, we controlled attention by our contrast discrimination task, which was identical for each image category. Importantly, this task focused the subjects' attention on the images, which may increase both the gain and specificity of the neural population representing the image attributes (Murray & Wojciulik, 2004). In addition, eye-movements are not significantly different when viewing these kinds of images (Dumoulin & Hess, 2006). Therefore, we believe that sensory, rather than attentional or eye-movement related, processes are underlying our results.

The finding that circular patterns elicit stronger activity in V4 is supported by both stereotaxic and VOI analysis (Figs. 2 and 3) and is consistent with previous studies reporting stronger neuronal responses to concentric shapes in macaque V4 (Gallant et al., 1993, 1996) and human V4 (Wilkinson et al., 2000) than to parallel (1D) patterns. Different responses to concentric versus parallel structure in images may not necessarily be mediated by circular structure, since other structure differences associated with circular but not parallel structures may underly the differential responses, such as orientation contrast of neighboring regions (Allman et al., 1985; Dumoulin & Hess, 2006; Fitzpatrick, 2000; Kastner et al., 2000; Williams et al., 2003; Zenger-Landolt & Heeger, 2003) or curvature (Ito & Komatsu, 2004; Pasupathy & Connor, 1999, 2001, 2002; Pollen et al., 2002). Our study adds to the previous studies by showing that the stronger signals to circular patterns are not due to orientation contrast or curvature inherent to circular patterns. Therefore, our results support the hypothesis that concentric (circular) shape processing is an important aspect of intermediate shape processing (Gallant et al., 1993, 1996; Wilkinson et al., 2000; Wilson et al., 1997; Wilson & Wilkinson, 1998).

Acknowledgments

The authors wish to thank Rebecca Achtman, Xingfeng Li, and the subjects for their help. This research was

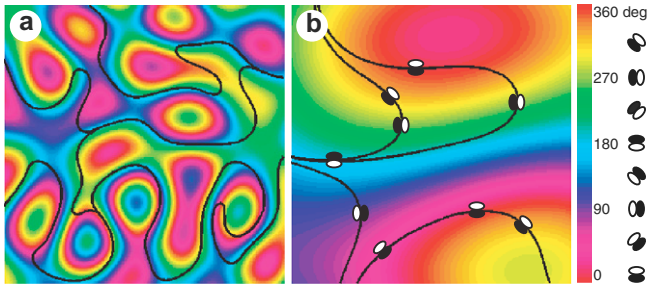

Fig. 4. Examples of the smoothed "orientation" images used to create the flowfield images are shown, containing relatively high (a) and low (b) spatial frequencies. Four "paths" are traced through these orientation-images going through the centers of each quadrant (black lines). The paths are traced according to the underlying orientation information in the images. The paths illustrate that semi-randomly placed Gabors whose orientation is determined by these images will vary either rapidly with high curvature (a) or slowly with low curvature (b). For illustration some Gabors are placed in (b) at different locations along the drawn paths, in the actual flowfield images Gabors were semi-randomly placed.

supported by Canadian Institutes of Health Research (CIHR) Grant MOP-53346 to R.F.H.

Appendix A

The creation of the flowfield images are illustrated in Fig. 4. The orientations of the Gabors in the flowfield images were determined by a band-pass filtered (smoothed) random pixel array (orientation-image) scaled and wrapped to contain a uniform distribution of values between 0 and 360 degrees. This filtered orientation-image was then used as a 2D look-up table to determine the Gabor's orientation depending on the Gabor's *xy*-coordinates. Thus, this orientation-image will determine the rate of orientation change (smoothness) and ultimately the curvature of Gabors oriented according to this array.

For example, a high-pass filter will force the orientations of Gabors to vary rapidly across space with high curvature (Fig. 4a), whereas a low-pass filter will only allow the orientations of the Gabors to vary slowly across space with low curvature (Fig. 4b). In Fig. 4b, a few example Gabors have been placed on the traced paths, however in the actual experiment the Gabor's were semi-randomly placed. The peak frequency and width of the band-pass function was varied in order to match the orientation gradient in the flowfield Gabor array with the corresponding circular Gabor array.

References

Achtman, R. L., Hess, R. F., & Wang, Y.-Z. (2003). Sensitivity for global shape detection. *Journal of Vision, 3*, 616–624.

Allman, J., Miezin, F., & McGuinness, E. (1985). Stimulus specific responses from beyond the classical receptive field: neurophysiological mechanisms for local–global comparisons in visual neurons. *Annual Review of Neuroscience, 8*, 407–430.

Beauchamp, M. S., Cox, R. W., & DeYoe, E. A. (1997). Graded effects of spatial and featural attention on human area MT and associated motion processing areas. *Journal of Neurophysiology, 78*, 516–520.

Brainard, D. H. (1997). The psychophysics toolbox. *Spatial Vision, 10*, 433–436.

Brefczynski, J. A., & DeYoe, E. A. (1999). A physiological correlate of the "spotlight" of visual attention. *Nature Neuroscience, 2*, 370–374.

Cocosco, C. A., Zijdenbos, A. P., & Evans, A. C. (2003). A fully automatic and robust brain MRI tissue classification method. *Medical Image Analysis, 7*, 513–527.

Collins, D. L., Neelin, P., Peters, T. M., & Evans, A. C. (1994). Automatic 3D intersubject registration of MR volumetric data in standardized Talairach space. *Journal of Computer Assisted Tomography, 18*, 192–205.

Dakin, S. C., & Bex, P. J. (2002). Summation of concentric orientation structure: Seeing the glass or the window? *Vision Research, 42*, 2013–2020.

De Valois, R. L., & De Valois, K. K. (1988). *Spatial vision*. Oxford University Press.

Desimone, R., & Schein, S. J. (1987). Visual properties of neurons in area V4 of the macaque: Sensitivity to stimulus form. *Journal of Neurophysiology, 57*, 835–868.

Dumoulin, S. O., Bittar, R. G., Kabani, N. J., Baker, C. L., Jr., Le Goualher, G., Pike, G. B., et al. (2000). A new anatomical landmark for reliable identification of human area V5/MT: A quantitative analysis of sulcal patterning. *Cerebral Cortex, 10*, 454–463.

Dumoulin, S. O., & Hess, R. F. (2006). Modulation of V1 activity by shape: Image-statistics or shape-based perception? *Journal of Neurophysiology, 95*, 3654–3664.

Dumoulin, S. O., Hoge, R. D., Baker, C. L., Jr., Hess, R. F., Achtman, R. L., & Evans, A. C. (2003). Automatic volumetric segmentation of human visual retinotopic cortex. *Neuroimage, 18*, 576–587.

Engel, S. A., Rumelhart, D. E., Wandell, B. A., Lee, A. T., Glover, G. H., Chichilnisky, E. J., et al. (1994). FMRI of human visual cortex. *Nature, 369*, 525.

Fitzpatrick, D. (2000). Seeing beyond the receptive field in primary visual cortex. *Current Opinion Neurobiology, 10*, 438–443.

Gallant, J. L., Braun, J., & Van Essen, D. C. (1993). Selectivity for polar, hyperbolic, and cartesian gratings in macaque visual cortex. *Science, 259*, 100–103.

Gallant, J. L., Connor, C. E., Rakshit, S., Lewis, J. W., & Van Essen, D. C. (1996). Neural responses to polar, hyperbolic, and cartesian gratings in area V4 of the macaque monkey. *Journal of Neurophysiology, 76*, 2718–2739.

Gallant, J. L., Shoup, R. E., & Mazer, J. A. (2000). A human extrastriate area functionally homologous to macaque V4. *Neuron, 27*, 227–235.

Gandhi, S. P., Heeger, D. J., & Boynton, G. M. (1999). Spatial attention affects brain activity in human primary visual cortex. *Proceedings of the National Academy of Sciences of the United States of America, 96*, 3314–3319.

Hess, R., & Field, D. (1999). Integration of contours: New insights. *Trends in Cognitive Sciences, 3*, 480–486.

Hess, R. F., Wang, Y. Z., & Dakin, S. C. (1999). Are judgements of circularity local or global? *Vision Research, 39*, 4354–4360.

Hubel, D. H., & Wiesel, T. N. (1959). Receptive fields of single neurons in the cat's striate cortex. *Journal of Physiology, 148*, 574–591.

Hubel, D. H., & Wiesel, T. N. (1962). Receptive fields, binocular interactions, and functional architecture in the cat's visual cortex. *Journal of Physiology, 160*, 106–154.

Ito, M., & Komatsu, H. (2004). Representation of angles embedded witin contour stimuli in area V2 of macaque monkeys. *Journal of Neuroscience, 24*, 3313–3324.

Kanwisher, N., McDermott, J., & Chun, M. M. (1997). The fusiform face area: A module in human extrastriate cortex specialized for face perception. *Journal of Neuroscience, 17*, 4302–4311.

Kastner, S., Weerd, P. D., & Ungerleider, L. G. (2000). Texture segregation in the human visual cortex: A functional mri study. *Journal of Neurophysiology, 83*, 2453–2457.

Kovács, I., & Julesz, B. (1993). A closed curve is much more than an incomplete one: Effect of closure in figure-ground segmentation. *Proceedings of the National Academy of Sciences of the United States of America, 90*, 7495–7497.

Kurki, I., & Saarinen, J. (2004). Shape perception in human vision: Specialized detectors for concentric spatial structures? *Neuroscience Letters, 360*, 100–102.

Levi, D. M., & Klein, S. A. (2000). Seeing circles: What limits shape perception? *Vision Research, 40*, 2329–2339.

MacDonald, D., Kabani, N., Avis, D., & Evans, A. C. (2000). Automated 3-D extraction of inner and outer surfaces of cerebral cortex from MRI. *Neuroimage, 12*, 340–356.

Martinez, A., Anllo-Vento, L., Sereno, M. I., Frank, L. R., Buxton, R. B., Dubowitz, D. J., et al. (1999). Involvement of striate and extrastriate visual cortical areas in spatial attention. *Nature Neuroscience, 2*, 364–369.

Murray, S. O., & Wojciulik, E. (2004). Attention increases neural selectivity in the human lateral occipital complex. *Nature Neuroscience, 7*, 70–74.

O'Craven, K. M., Rosen, B. R., Kwong, K. K., Treisman, A., & Savoy, R. L. (1997). Voluntary attention modulates fMRI activity in human MT-MST. *Neuron, 18*, 591–598.

Pasupathy, A., & Connor, C. E. (1999). Responses to contour features in macaque area V4. *Journal of Neurophysiology, 82*, 2490–2502.

Pasupathy, A., & Connor, C. E. (2001). Shape representation in area V4: Position-specific tuning for boundary conformation. *Journal of Neurophysiology, 86*, 2505–2519.

Pasupathy, A., & Connor, C. E. (2002). Population coding of shape in are V4. *Nature Neuroscience, 5*, 1252–1254.

Pei, F., Pettet, M. W., Vildavski, V. Y., & Norcia, A. M. (2005). Event-related potentials show configural specificity of global form processing. *Neuroreport, 16*, 1427–1430.

Pelli, D. G. (1997). The Videotoolbox software for visual psychophysics: Transforming numbers into movies. *Spatial Vision, 10*, 437–442.

Pettet, M. W., McKee, S. P., & Grzywacz, N. M. (1998). Constraints on long range interactions mediating contour detection. *Vision Research, 38*, 865–879.

Pollen, D. A., Przybyszewski, A. W., Rubin, M. A., & Foote, W. (2002). Spatial receptive field organization of macaque V4 neurons. *Cerebral Cortex, 12*, 601–616.

Schiller, P. H., & Lee, K. (1991). The role of the primate extrastriate area V4 in vision. *Science, 251*, 1251–1253.

Sereno, M. I., Dale, A. M., Reppas, J. B., Kwong, K. K., Belliveau, J. W., Brady, T. J., et al. (1995). Borders of multiple visual areas in humans revealed by functional magnetic resonance imaging. *Science, 268*, 889–893.

Sled, J. G., Zijdenbos, A. P., & Evans, A. C. (1998). A non-parametric method for automatic correction of intensity non-uniformity in MRI data. *IEEE Transactions on Medical Imaging, 17*, 87–97.

Somers, D. C., Dale, A. M., Seiffert, A. E., & Tootell, R. B. H. (1999). Functional MRI reveals spatially specific attentional modulation in human primary visual cortex. *Proceedings of the National Academy of Sciences of the United States of America, 96*, 1663–1668.

Talairach, J., & Tournoux, P. (1988). *Co-planar stereotaxic atlas of the human brain*. New York: Thieme.

Wilkinson, F., James, T. W., Wilson, H. R., Gati, J. S., Menon, R. S., & Goodale, M. A. (2000). An fMRI study of the selective activation of human extrastriate form vision areas by radial and concentric gratings. *Current Biology, 10*, 1455–1458.

Wilkinson, F., Wilson, H. R., & Habak, C. (1998). Detection and recognition of radial frequency patterns. *Vision Research, 38*, 3555–3568.

Williams, A. L., Singh, K. D., & Smith, A. T. (2003). Surround modulation measured with functional MRI in the human visual cortex. *Journal of Neurophysiology, 89*, 525–533.

Wilson, H. R., & Wilkinson, F. (1998). Detection of global structure in glass patterns: Implications for form vision. *Vision Research, 38*, 2933–2947.

Wilson, H. R., Wilkinson, F., & Asaad, W. (1997). Concentric orientation summation in human form vision. *Vision Research, 37*, 2325–2330.

Worsley, K. J., Liao, C., Aston, J., Petre, V., Duncan, G. H., Morales, F., et al. (2002). A general statistical analysis for fMRI data. *Neuroimage, 15*, 1–15.

Worsley, K. J., Marrett, S., Neelin, P., Vandal, A. C., Friston, K. J., & Evans, A. C. (1996). A unified statistical approach for determining significant signals in images of cerebral activation. *Human Brain Mapping, 4*, 58–73.

Zenger-Landolt, B., & Heeger, D. J. (2003). Response suppression in V1 agrees with psychophysics of surround masking. *Journal of Neuroscience, 23*, 6884–6893.